Efficient and Secure μ-Training and μ-Fine-Tuning for TinyML Optimization and Personalization at the Edge

Zhaojing Huang[1]*, Leping Yu[1], Luis Fernando Herbozo Contreras[1], Omid Kavehei[1]

Abstract

This study introduces a novel approach for training and fine-tuning machine learning models for bio-signal data analysis on edge medical devices. The technique can be used in all physiological signals, and in this paper, we used electrocardiogram (ECG) signals as a case example to demonstrate its capability. The proposed methodology combines full training and a novel technique termed μ-Training, in which the encoder and decoder layers of the tiny model are frozen. In contrast, the middle layer weights remain trainable. We investigate the effectiveness of this approach across different stages, including full training, μ-Training, and μ-Fine-Tuning. The model's performance is evaluated using both in-sample data from the Telehealth Network of Minas Gerais (TNMG) dataset and an out-of-sample test on the China Physiological Signal Challenge 2018 (CPSC) dataset, with the results demonstrating that the combined training approach performs similarly to or better than traditional full training and fine-tuning while providing significant advantages in computational efficiency. Furthermore, the model is deployed on an edge device for μ-Fine-Tuning, showcasing its effectiveness even under resource-constrained conditions. For demonstration and deployment purposes, we used Radxa Zero hardware, while a range of other edge devices can be used. The results demonstrate that the proposed method outperforms traditional approaches, improving computational efficiency and resource utilization, making it a promising solution for real-time bio-signal processing on edge devices.

Keywords: Edged device, Fine-tuning, Secure AI, TinyML, Training method, Heart abnormalities, Bio-signals.

1 Introduction

One of the key challenges in the medical domain is developing models that can be personalized for individual patients. To achieve this, models need to adapt to new personal data. However, when it comes to edge devices, their often severely limited computational and memory capacity makes local fine-tuning on new data impractical. Traditionally, this challenge is addressed by transferring data to external servers for processing [1]. However, this raises significant data security concerns, as such transfers are vulnerable to hacking and unauthorized access [2].

An alternative approach is Federated Learning (FL), which exchanges gradients instead of raw data to mitigate privacy risks [3]. However, recent studies have shown that even gradients can be exploited to reconstruct sensitive data [4, 5]. Moreover, transferring either data or gradients can rapidly drain the device's battery (if battery-powered), as data transmission, which often has to be wireless, consumes substantial energy [6].

Our previous work introduced a novel method for fine-tuning large foundational models without requiring data or gradient transfer [7]. This approach facilitates fine-tuning large models directly on resource-limited devices, enhancing data security and efficiency. However, recent advancements in machine learning have led to the development of smaller models that can deliver performance comparable to larger models [8]. Despite their smaller model size, fine-tuning these models on resource-constrained edge devices poses a significant challenge.

Huang et al. [7]'s μ-Trainer, initially designed for fine-tuning larger models, offers valuable insights into improving the efficiency of fine-tuning smaller models. This approach allows for more efficient fine-tuning in resource-constrained environments. A key concept in μ-Trainer is to focus knowledge condensation in specific model layers, freeing up other layers to better adapt to new information. Building on this idea, we aim to develop a new methodology tailored for fine-tuning smaller models for personalized use, emphasizing maximizing resource efficiency. To demonstrate the effectiveness of this approach, we utilized one of our previously developed tiny models on electrocardiogram (ECG) data [8], highlighting its potential for medical applications.

ECG is a critical diagnostic tool for assessing cardiac activity, providing information about the electrical signals generated by the heart muscle during heart movement. It plays a pivotal role in detecting cardiac irregularities, aiding in the early diagnosis of heart conditions, and mitigating the risk of stroke [9]. The challenges of resource-constrained environments, data privacy, and security are particularly pressing in the AI-driven biomedical field. Striking a balance between leveraging data for medical advancements and safeguarding individual privacy is crucial. Addressing these challenges requires a multidisciplinary approach, combining several domains of expertise such as AI, healthcare system processes, and legal

* Corresponding author.

[1] Z. Huang, L. Yu, L. Herbozo, and O. Kavehei are with the School of Biomedical Engineering, The University of Sydney, NSW 2008, Darlington, Australia. (email: zhaojing.huang@sydney.edu.au)

frameworks to mitigate privacy risks and serious consequences for patients, staff or entities involved [10]. Our proposed method directly addresses this critical issue, as envisioned in Fig. 1.

Figure 1: The vision of this work is to develop a method for training and fine-tuning small yet accurate machine learning models on personal data, enabling secure model personalization while enhancing efficiency for on-device fine-tuning. This approach is particularly crucial in the medical domain, where data security and resource efficiency are paramount.

With the proliferation of Internet of Things (IoT) applications and the potential integration with machine learning at the edge, the need for personalization at the edge is expected to grow. The integration of IoT and edge-based Artificial Intelligence (AI) offers compelling benefits, such as ultra-low latency, strengthened data security, enhanced privacy protections, and significant cost reductions [11]. This study focuses on a medical application case and aims to expand its application beyond the medical domain to other fields of IoT.

1.1 Background

Building on the μ-Trainer framework [7], we propose μ-Training and μ-Fine-Tuning tailored specifically for tiny models. This new method extends the core idea of μ-Trainer by enabling training and fine-tuning to focus on specific model parts, optimizing computational and memory efficiency. Additionally, this approach aims to enhance the performance of models trained and fine-tuned using this methodology.

1.1.1 Tiny Machine Learning (TinyML)

Our previous works investigated the potential of tiny models that achieve strong performance while maintaining a compact size in terms of weights and parameters. We identified the Diagonal State Space Sequence (S4D) model as highly effective for processing sequential data [12, 13]. Additionally, we explored the capabilities of specialized neurons, such as Neural Circuit Policies (NCP) [14, 15, 16] and Kolmogorov-Arnold Networks (KAN) [17, 18], both of which demonstrated promising results. Building on these findings, we successfully integrated the S4D model with NCP neurons to create an extremely compact model that delivers strong performance on time-series data [8]. For this study, we will utilize this compact, lightweight model to demonstrate the effectiveness of our proposed methodology. The model can be divided into 3 primary layers: the encoder, the S4D layer, and the decoder. Further details about the model's architecture will be provided in Section 2.1.

1.1.2 Privacy and Data Security

Several approaches, such as FL and server-based data upload, have been developed for fine-tuning models [19]. FL has been widely adopted in fields like electronic health record management, medical image processing, and remote health monitoring [3].
However, risks of user data leakage remain. Zhu et al. [4] introduced Deep Leakage from Gradients (DLG), a method capable of reconstructing training inputs and labels directly from gradients. Similarly, Boenisch et al. [5] demonstrated vulnerabilities in FL, showing that even when protected by Distributed Differential Privacy (DDP) and Secure Aggregation (SA), FL remains susceptible to breaches. These findings highlight that FL, despite its advancements, does not fully guarantee user privacy. Therefore, innovative methods prioritizing user privacy and robust data security are essential for advancing edge AI systems.

1.1.3 Personalized Model Adaptation

Personalization based on specific user data is essential to enhance the suitability of models for individual users.
However, transmitting data outside the device is energy-inefficient, and combined with privacy and data security concerns, on-device fine-tuning emerges as a feasible solution. These challenges highlight the need for local, on-device training solutions [20].

1.2 Overview of the Proposed Approach

The proposed method, outlined in Fig. 2 and Algorithm 1, is structured into three steps to fine-tune a small model for more personalized usage while maintaining user privacy. Personal data is retained on the device throughout this process, mitigating potential privacy concerns. At no stage is information such as input data batches x, true labels y, or gradients ∇W transferred beyond the device. Fine-tuning is performed locally using privately collected personal data, and the iterative processes for each step are described as follows.
In Step 1, the model undergoes full training on an external server, where all weights are updated through the

standard backpropagation process. The weights are adjusted using the Eq. 1.

$$W_{t+1} = W_t - \alpha \nabla_{W_t} \mathcal{L}(W_t, x, y) \ , \tag{1}$$

where W_t represents the model weights at iteration t, α is the learning rate, $\nabla_{W_t}\mathcal{L}$ denotes the gradient of the loss function $\mathcal{L}$, and x, y are the input data and labels, respectively.

In Step 2, during μ-Training, the encoder and decoder layers are frozen, and only the middle S4D layer remains trainable. The updated weights of the S4D layer are computed as Eq. 2.

$$W_{\text{S4D},t+1} = W_{\text{S4D},t} - \alpha \nabla_{W_{\text{S4D},t}} \mathcal{L}(W_{\text{S4D},t}, x, y) \ . \tag{2}$$

Here, $W_{\text{S4D},t}$ denotes the weights of the trainable S4D layer, while the encoder and decoder weights remain fixed.

In Step 3, during μ-Fine-Tuning, the middle S4D layer is frozen, and the encoder and decoder layers become trainable to allow the model to adapt to new, unseen data. The weights are updated using Eq. 3.

$$W_{\text{enc/dec},t+1} = W_{\text{enc/dec},t} - \alpha \nabla_{W_{\text{enc/dec},t}} \mathcal{L}(W_{\text{enc/dec},t}, x, y) \tag{3}$$

where $W_{\text{enc/dec},t}$ represents the trainable weights of the encoder and decoder layers during fine-tuning.

Algorithm 1 μ-Training and μ-Fine-Tuning Process

Step 1: Full Training
Train the tiny model M on a large dataset $\mathcal{D}_{\text{large}}$ by minimizing the loss $\mathcal{L}(M(\mathcal{D}_{\text{large}}), y)$
Update all weights $\theta = [\theta_{\text{enc}}, \theta_{\text{mid}}, \theta_{\text{dec}}]$
Step 2: μ-Training
Freeze the weights in the encoder and decoder: θ_{enc}, θ_{dec}
Train the middle layer θ_{mid} on the dataset $\mathcal{D}_{\text{large}}$ by minimizing $\mathcal{L}(M_\mu(\mathcal{D}_{\text{large}}), y)$
Step 3: μ-Fine-Tuning
Freeze the middle layer θ_{mid} and unfreeze the encoder and decoder weights: θ_{enc}, θ_{dec}
while Fine-tuning on the personal dataset $\mathcal{D}_{\text{personal}}$ **do**
  Minimize the personal loss $\mathcal{L}_{\text{personal}}(M_\mu(\mathcal{D}_{\text{personal}}), y)$
end while
Update the model M with fine-tuned weights $\theta_{\text{enc}}^{M_\mu}$ and $\theta_{\text{dec}}^{M_\mu}$
return Fine-tuned Personal Model M

The methodology is further detailed in Section 4. Two datasets were employed to simulate the experimental process while ensuring minimal use of personal data. The first dataset is the original training data for pre-training the model. In contrast, the second dataset is specifically designed to evaluate the effectiveness of the proposed fine-tuning approach. Comprehensive descriptions of these datasets, including their characteristics and relevance to the experiments, are provided in Section 3.

Compared to conventional methods, where data is sent outside the device for external fine-tuning, and Federated Learning (FL), where gradients are shared outside the device for global aggregation, our proposed method significantly advances in privacy protection, personalization, and on-device training. A qualitative comparison is provided in Table 1, which underscores the unique contributions of this work in comparison with other approaches that share the same aim.

Table 1: Comparison of various methodologies ($\surd$: Yes; $\times$: No; –: Challenging)

	Privacy	Personalize	On-device Learning	Compute Efficiency
Conventional	$\times$ †	$\surd$	– ‡	$\times$
FL	$\times$ [4]	– [5]	–	$\times$
Proposed	$\surd$	$\surd$	$\surd$	$\surd$

† Transmitting user data externally presents substantial privacy risks, as it exposes sensitive information to potential unauthorized access by malicious actors, such as hackers, who could exploit this direct access.

‡ Edge devices typically lack the necessary memory and computational power for full model training or fine-tuning, a standard practice in conventional methods.

2 Prerequisite

2.1 Tiny Diagonal State Space Model

The Tiny Diagonal State Space Model (TDSSM) is a simplified and computationally efficient approach to modelling dynamical systems [8]. The model builds on the standard state-space framework, which describes how the system's state evolves over time and how the internal state relates to observed measurements [8]. In the TDSSM, these equations are streamlined to minimize computational and memory demands, making the model suitable for edge devices and real-time applications [8].

One defining characteristic of the Tiny Diagonal State Space Sequence (S4D) Model is using diagonal matrices for key components such as the state transition or observation matrices [12]. This diagonal assumption greatly reduces computational complexity as operations like matrix multiplications and inversions become simpler and more efficient. While diagonalization limits the model's expressiveness compared to general state-space models, it is sufficient for capturing essential patterns in many practical applications [8]. The S4D model is a model that has excellent performance on large amounts of data, which is suitable for complex datasets [12, 13]. The Neural Circuit Policy (NCP) decoder is utilized in this model. It draws inspiration from the nervous system of the nematode Caenorhabditis elegans, which features a highly efficient network of neurons that facilitate enhanced communication and coordination. This design enables the NCP decoder to achieve efficient and robust processing capabilities [14, 15, 16]. The complete model structure

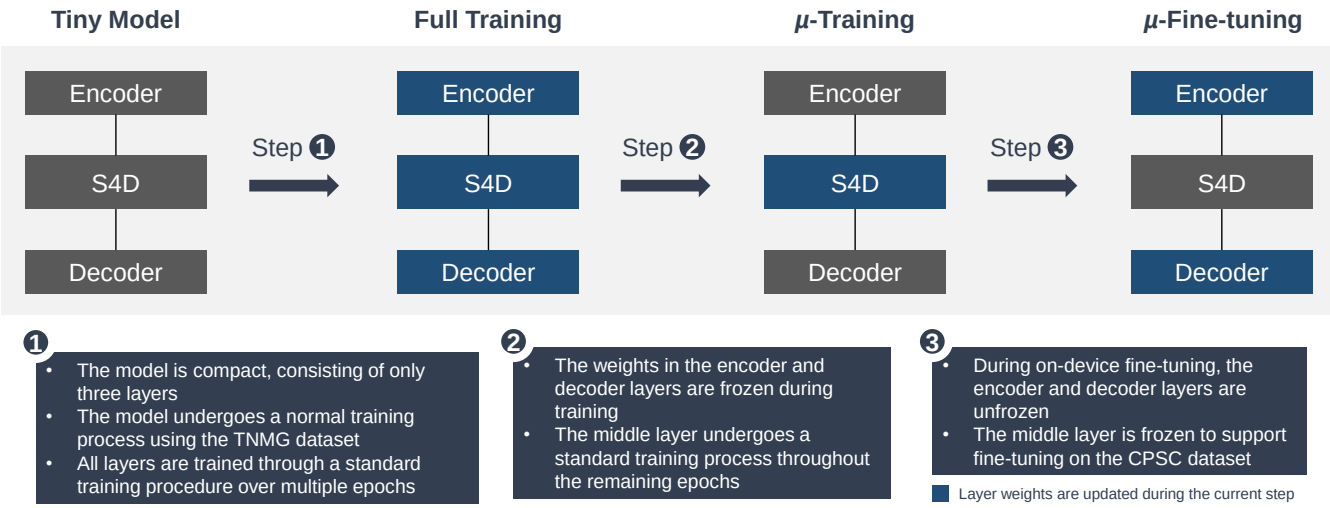

Figure 2: The chart provides a detailed overview of the methodology, divided into three distinct steps. Step 1 - Full Training: In this step, the model operates in full training mode, where all weights are updated through the standard training process. Step 2 - μ-Training: During μ-Training, the weights in the encoder and decoder are frozen, while the middle S4D layer remains trainable. Step 3 - μ-Fine-Tuning: In the final step, the trained model undergoes μ-Fine-Tuning on the device. Here, the middle S4D layer is frozen while the encoder and decoder are set to be trainable, enabling the model to adapt its weights to new, unseen data. Green highlights in the chart indicate the layers where weights are updated during each respective step.

is shown in Fig. 3.

For cardiac abnormality detection, as explored in the referenced paper, the TDSSM provides an efficient way to model the dynamics of cardiac signals, such as electrocardiograms (ECGs) [8]. The approach can detect abnormalities potentially on low-power wearable devices, by leveraging the model's simplicity and low computational footprint. This makes it a promising tool for portable health monitoring systems [8].

2.2 μ-Trainer

μ-Trainer is a novel method that was developed to enable the training of large-scale machine learning models on resource-constrained devices. This method utilizes knowledge distillation, which is performed using a "student" model trained to replicate the behaviour and knowledge of a larger, more complex "teacher" model. By focusing on efficient knowledge transfer, μ-Trainer ensures that even resource-limited devices can benefit from the capabilities of large machine learning models [7].

One of the key features of μ-Trainer is the ability to compress knowledge. The method selectively transfers the most relevant information from the teacher model to the student model while eliminating redundant or unnecessary knowledge. This approach allows the student model to achieve performance levels close to the teacher model but with a significantly smaller computational and memory footprint [7]. By utilizing the μ-Trainer for fine-tuning, it ensures that the data and gradients are not communicated outside the device, thereby preserving privacy [4, 5].

To optimize training for edge devices, μ-Trainer utilized dynamic layer freezing, a strategy where less critical layers of the model are frozen during training. This reduces computational demands without significantly affecting the model's accuracy, making it particularly suited for edge applications [7].

Another distinctive feature of μ-Trainer is its use of progressive knowledge transfer. This training strategy involves transferring knowledge from the student model to the larger one and creating a new student model to adapt to newer data. This process is repeated in a loop, enabling continuous improvement of the larger model over time [7].

2.3 μ-Training and μ-Fine-tuning Tiny Models

The μ-Trainer was initially designed to enhance the security of fine-tuning large foundational models locally within resource-constrained environments. However, its underlying concept could also benefit the personalization of smaller models in the medical domain, an area of critical importance. Beyond ensuring the security of personal data, the μ-Trainer can potentially improve the efficiency of model personalization and fine-tuning processes. The core idea of the μ-Trainer is to enable one part of the model to focus on learning specific data features while allowing another part of the model greater flexibility to adapt to new data. This study explores how these benefits can be applied to fine-tune a smaller model (TDSSM) we previously developed and tested. We have designed the technique to enable the small model to undergo a

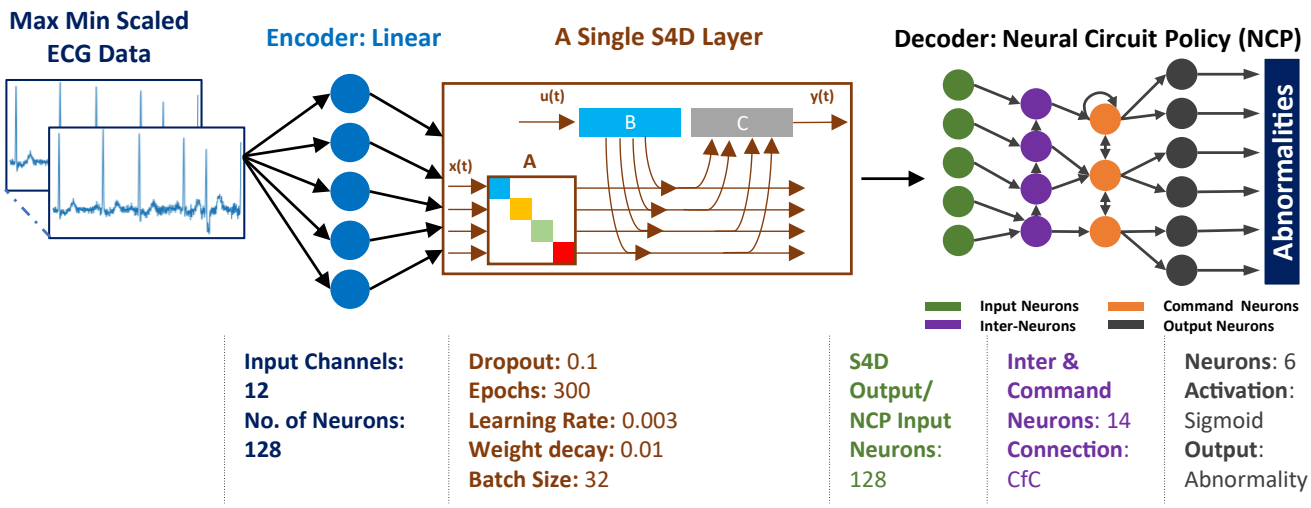

Figure 3: Huang et al. [8]'s Tiny Diagonal State Space Model features a single linear encoder, single S4D layer, and simple NCP neurons serving as the decoder. Adapted from Huang, Z., et al. APL Mach. Learn. 2, 026112 (2024). `https://doi.org/10.1063/5.0191574`. Licensed under CC BY 4.0.

standard training process, followed by μ-Training and μ-Fine-Tuning on new data, to achieve effective personalization.

3 Datasets

The evaluation of the proposed approach in this study was carried out using two separate datasets. The first dataset, called the Telehealth Network of Minas Gerais (TNMG) dataset [21], is tailored for detecting abnormalities in both rhythm and morphology within 12-lead ECG recordings. This dataset served as the training ground for the model presented in this work.
The second dataset, the CPSC dataset, was created for the China Physiological Signal Challenge 2018 [22]. It consists of labeled abnormality data for 12-lead ECG signals and was utilized during the fine-tuning stage to mimic scenarios where new and unfamiliar data are encountered.

3.1 TNMG

The TNMG dataset consists of 2,322,513 distinct labeled samples, each representing 10 seconds of 12-lead ECG data. These samples cover six different types of abnormalities: Atrial Fibrillation (AF), First Degree Atrioventricular Block (1dAVb), Left Bundle Branch Block (LBBB), Right Bundle Branch Block (RBBB), Sinus Bradycardia (SB), and Sinus Tachycardia (ST) [21]. The sampling rate for this dataset is 40 Hz.
A balanced subset was created by randomly selecting 3,000 samples for each of the six abnormality types, as well as an additional 3,000 samples representing healthy ECG readings, resulting in a total of 21,000 samples for model training. In cases where patients exhibited multiple abnormalities, any additional samples required to reach the subset size of 21,000 were randomly chosen from the full TNMG dataset. Further details on these abnormalities can be found in Table 2.

The dataset was standardized to a fixed length of 4,096 readings to ensure uniformity in analysis and modeling. Readings exceeding this length were truncated to streamline data processing and facilitate comparison. Fig. 4 illustrates the balanced gender distribution in the resampled dataset, enhancing generalizability and supporting robust analysis. Furthermore, the dataset reflects the age distribution of the general population, highlighting its relevance for age-related studies. Additionally, the balanced representation of different abnormalities in the dataset enhances the model's learning efficiency and overall performance [29].

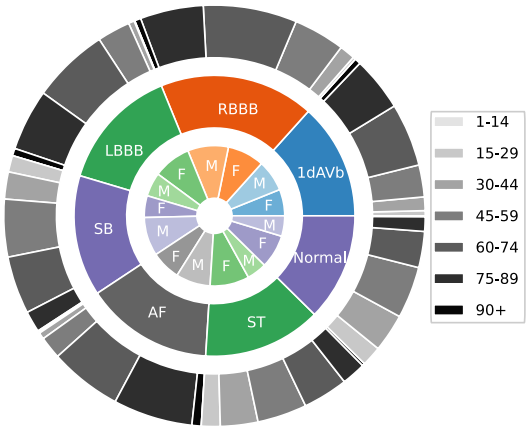

Figure 4: The TNMG subset is a well-balanced dataset comprising six types of abnormalities and features a higher proportion of older patients, aligning with the demographics of the general population. Adopted from Huang, Z., et al. J. of Cardiovasc. Trans. Res. (2024). `https://doi.org/10.1007/s12265-024-10504-y`. Licensed under CC BY 4.0.

Table 2: Classification of Abnormalities in the TNMG Dataset with Descriptions.

Abnormality	Description
Atrial Fibrillation (AF)	A common arrhythmia characterized by rapid and irregular heartbeats, leading to an irregular ventricular response [23].
Sinus Tachycardia (ST)	A condition where the heart rate exceeds 100 beats per minute, originating from the sinoatrial node. It can result from various physiological or pathological conditions [24].
Sinus Bradycardia (SB)	Defined as a heart rate of fewer than 60 beats per minute, with impulses originating from the sinoatrial node. It can be normal in athletes or indicate underlying pathology [25].
Left Bundle Branch Block (LBBB)	A delay or blockage in the left bundle branch of the heart's conduction system, causing the left ventricle to contract later than the right [26].
Right Bundle Branch Block (RBBB)	A condition where there's a delay or blockage in the right bundle branch, leading to delayed right ventricular contraction [27].
First Degree Atrioventricular Block (1dAVb)	Characterized by a prolonged PR interval exceeding 200 ms on an ECG, indicating delayed conduction through the atrioventricular node [28].

3.2 CPSC

The CPSC dataset comprises 12-lead ECG recordings ranging from 6 to 60 seconds in duration, sampled at a rate of 500 Hz. To ensure compatibility with the CPSC dataset, the TNMG data was resampled to match this rate specifically for training purposes. The CPSC dataset includes ECGs from patients diagnosed with various cardiovascular conditions, accompanied by precise annotations for abnormalities. In total, the dataset covers eight distinct types of abnormalities.

This dataset, previously unused in training the model, serves as a benchmark to evaluate the fine-tuning potential of the proposed methods. While the CPSC dataset contains eight abnormality classes, four overlap with those in the TNMG dataset, making them the focus for fine-tuning evaluation. The selected abnormalities for assessment include Atrial Fibrillation (AF), Left Bundle Branch Block (LBBB), Right Bundle Branch Block (RBBB), and First Degree Atrioventricular Block (1dAVb). The remaining abnormalities—Premature Atrial Contraction (PAC), Premature Ventricular Contraction (PVC), ST-segment Depression (STD), and ST-segment Elevation (STE)—were excluded from this study.

As part of data preparation, entries with missing values were removed, resulting in a final dataset of 6,877 unique ECG tracings. All recordings were standardized to 4,096 readings for consistency, with excess data truncated during the cleaning process. Fig. 5 illustrates the distribution of abnormalities within the CPSC dataset.

Analysis of the CPSC dataset revealed a gender imbalance, with a higher proportion of male patients than females. However, the age distribution aligns closely with the general population, showing a higher representation of older individuals. While most abnormalities are evenly represented, a slight under-representation of LBBB was observed compared to other abnormalities.

4 Methods

To evaluate the feasibility of our proposed technique, we designed a comprehensive experimental methodology outlined in Fig. 2. The process follows the steps depicted in the figure. This methodology is divided into three key phases, which will be discussed in detail in the following subsections.

4.1 Step 1 - Full Training

The first step involves training the TDSSM, adapted from the work of Huang et al. [8].

This model is exceptionally lightweight, with only 58,509 parameters and a total size of 242 KB. Despite its compact design, the model achieves performance levels comparable to larger models [8]. The training process spanned a total of 300 epochs. The TNMG subset is utilized during the training phase, with the ECG data subjected to min-max scaling to normalize its range, thereby improving the model's generalizability and performance [8].

A batch size of 32 was employed throughout the training to ensure efficient data processing. The training regimen utilized a learning rate of 0.003, optimized with the Adam optimizer and binary cross-entropy loss function. We incorporated the Cosine Annealing Learning Rate Scheduler to enhance training dynamics, gradually reducing the learning rate following a cosine annealing pattern. This approach facilitates smoother convergence, avoiding abrupt learning rate changes that could destabilize training.

The training process was divided into two phases: *Full training* and *μ-Training*. All model layers and weights were trained in a standard manner during full training. In contrast, μ-Training involved a more targeted training strategy. Various combinations of full training and μ-Training were explored to evaluate the performance of the proposed technique. Notably, the total number of epochs for both phases combined was maintained at 300.

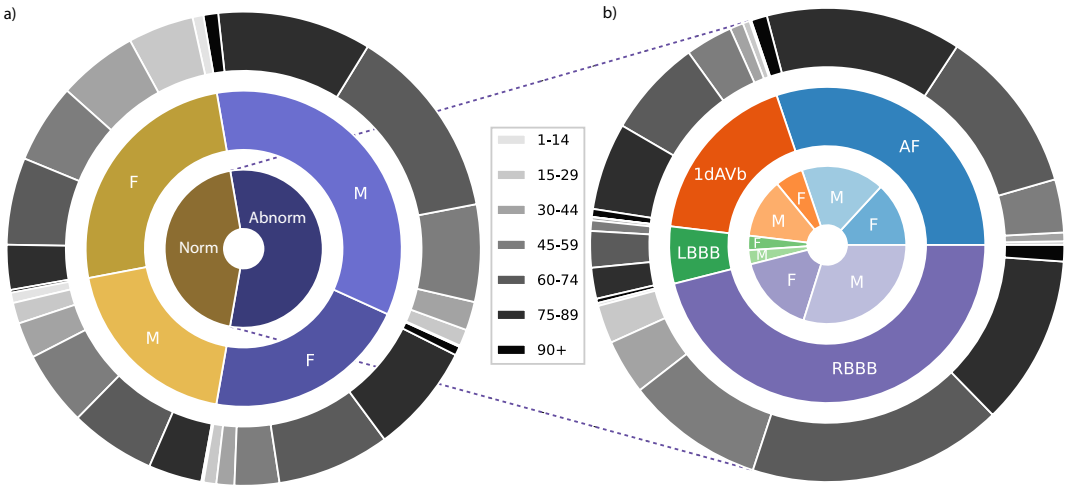

Figure 5: a) Distribution of patients with studied abnormalities versus those with normal ECG readings or other abnormalities in the CPSC dataset. b) Detailed breakdown of specific abnormalities is also shown. Adapted from Huang, Z., et al., J. of Cardiovasc. Trans. Res. (2024). `https://doi.org/10.1007/s12265-024-10504-y`. Licensed under CC BY 4.0.

4.2 Step 2 - μ-Training

The second step focuses on μ-Training, a specialized phase designed to refine the model while preserving the integrity of specific components. During μ-Training, the weights in the encoder and decoder layers are frozen, meaning these layers retain their pre-trained parameters from the previous step without further updates. Instead, all training updates are concentrated solely on the middle layer, which, in this case, is the S4D layer, comprising 49,920 weights out of the total 58,509. The μ-Training process is conducted on the TNMG dataset, also utilized during the full training phase.

This targeted approach allows the S4D layer to adapt more effectively to the training data while maintaining the structural stability provided by the frozen layers. By limiting updates to a single layer, μ-Training reduces computational overhead and enhances the model's ability to generalize without overfitting.

The entire training process, including both full training and μ-Training, is designed to conclude at 300 epochs. μ-Training occupies the remaining epochs after the initial full training phase, ensuring a seamless transition from broad training across all layers to a more focused refinement of the S4D layer. This methodical division aims to optimize the model's performance, balancing efficiency and accuracy.

4.3 Step 3 - μ-Fine-tuning

After completing the full training and μ-Training phases, the model undergoes the μ-Fine-Tuning process. Unlike the μ-Training phase, where only the middle S4D layer was updated, μ-Fine-Tuning freezes the S4D layer and allows only the encoder and decoder layers to adjust their weights. This strategic adjustment enables the model to adapt to new data while preserving the specialized functionality of the S4D layer. The encoder and decoder layers contain 8,589 weights, which account for approximately 14.68% of the total weights.

While the fine-tuning process shares similarities with the training procedure, it is limited to just 50 epochs to ensure rapid adaptation and computational efficiency. For this phase, a small, balanced subset of the CPSC dataset replicates real-world scenarios where the model must adapt to new, personalized data. Using a balanced dataset has been demonstrated to enhance personalization performance [7], making it an ideal approach for optimizing the model's effectiveness in individual applications. As the CPSC and TNMG datasets contain different classes of abnormalities, the loss function must be redesigned to account for these differences. This ensures that irrelevant classes do not interfere with the fine-tuning results.

To verify the effectiveness of the proposed technique, the model is also deployed onto an edge device. For this study, we utilized the Radxa Zero, a compact hardware platform powered by the Amlogic 905Y2 processor. This processor features a 64-bit Advanced RISC Machine (ARM) architecture and supports up to 4 GB of 32-bit memory, making it suitable for lightweight, resource-efficient deployment.

4.4 Evaluation Metrics

Evaluation metrics are indispensable for facilitating meaningful comparisons of model performance. The true and false detection threshold is set at 0.5 throughout the work. Precision (P), as defined in Eq 4, evaluates the accuracy of positive predictions, while recall (R), described in Eq 5, measures the model's effectiveness in identifying true positive cases. The F1-score (F_1), shown in Eq 6, combines precision and recall into a single metric, balancing their trade-off and offering a well-rounded assessment of the model's predictive capabilities.

$$P = \frac{TP}{FP + TP} \tag{4}$$

$$R = \frac{TP}{FN + TP} \tag{5}$$

$$F_1 = 2 \times \frac{R \times P}{R + P} \tag{6}$$

The Area Under the Receiver Operating Characteristic Curve (AUROC) is a key metric that evaluates a model's ability to distinguish between positive and negative cases across different threshold values, making it particularly useful in binary classification tasks.

Evaluation metrics such as the F1-score, precision, recall, and AUROC are crucial for evaluating the performance of machine learning models, particularly in applications like anomaly detection in binary classification tasks. These metrics comprehensively assess a model's ability to distinguish between different classes accurately.

5 Experiment

Since the entire training and μ-Training processes are interdependent within the overall training framework, the experiments are structured into two distinct phases. The first phase emphasizes the comprehensive training process, while the second focuses on the on-device fine-tuning aspect.

5.1 Phase 1 - Training Process (Full Training & μ-Training)

The primary objective of this phase is to determine the optimal allocation of epochs between the full-training period and the μ-Training period, identifying the most effective breakdown for each stage of the training process. The training process was configured to run for 300 epochs on the balanced TNMG subset, following the framework outlined in our previous work [8]. However, the proposed approach incorporates alternating full training and μ-Training phases. As the optimal allocation of epochs between these modes remains uncertain, we explored various combinations to determine the most effective distribution for maximizing model performance. Training models with various configurations systematically compared their performance, enabling us to determine the most suitable μ-Training strategy for achieving optimal results.

5.2 Phase 2 - μ-Fine-tuning Process

The subsequent fine-tuning experiment was conducted to simulate real-world scenarios where models are adapted to new, personalized data. The CPSC dataset was utilized to evaluate the fine-tuning capabilities of the trained models. In line with previous research indicating that fine-tuning on a balanced dataset yields optimal results [7], a subset of 1,000 samples was extracted from the CPSC dataset. This subset consisted of 200 samples each for the four shared abnormalities between the TNMG and CPSC datasets, along with 200 samples representing healthy data.

Only the shared abnormalities between the two datasets were considered throughout the fine-tuning process. The differences in abnormalities were carefully managed, with specific measures implemented to ensure that the unused abnormalities in the CPSC dataset did not interfere with the loss calculation. This approach ensured that the fine-tuning process remained focused and accurate.

For additional insight, one model was selected for fine-tuning directly on the Radxa Zero device, enabling a real-world evaluation of edge device performance compared to Graphics Processing Unit (GPU) based fine-tuning.

The fine-tuned models, trained over 50 epochs, were assessed on both the CPSC dataset to measure performance improvements on new, unseen data and the test set of the TNMG dataset to evaluate their impact on the original data domain. A comparative analysis was performed to gauge the effectiveness and adaptability of the proposed fine-tuning technique.

6 Results

This section presents the experiments' results, following the sequence outlined in the previous section.

6.1 Training Process

During the training phase, the TDSSM undergoes two distinct modes: full training and μ-Training. Initially, the model is set to full training mode, where all weights are updated through the standard training process. Following this, the model transitions to μ-Training mode, where the weights in the encoder and decoder layers are frozen, while the middle layer weights remain trainable.

The entire training process spans 300 epochs, consistent with previous model training [8]. To evaluate different configurations, we varied the allocation of epochs between full training and μ-Training. Specifically, the full training epochs were set to 0, 50, 100, 150, 200, 250, and 300, with the remaining epochs assigned to μ-Training. The details of the training process for these combinations of full training and μ-Training are illustrated in Fig. 6. The combination of 0 epochs of full training and 300 epochs of μ-Training yielded unsatisfactory results and has been excluded from the chart and subsequent analyses.

After completing the full training and μ-Training processes, the model is evaluated using the test dataset from the TNMG subset, which was part of the training process. Additionally, the model's performance is assessed on the CPSC dataset, serving as unseen data, to evaluate its generalization ability. Fig. 7a) the average F1 score and AUROC are presented, showcasing the model's performance on the TNMG test set and the CPSC dataset.

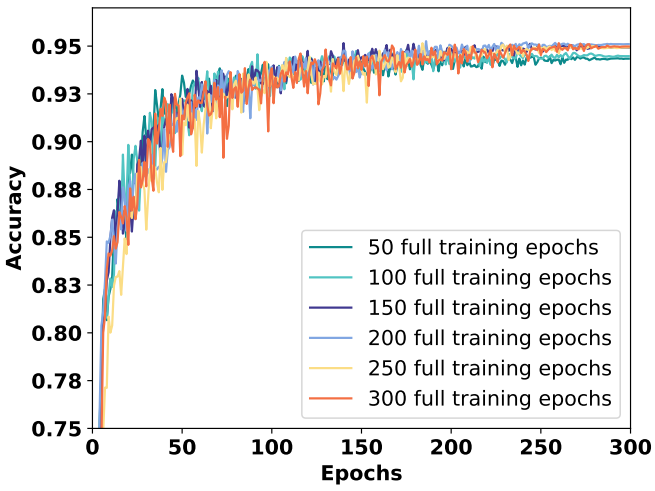

Figure 6: The accuracy evaluation across the entire training process for various combinations of full training and μ-Training.

Table 3 provides a detailed breakdown of the model's performance on the TNMG test data for each type of abnormality.
Table 4 presents a detailed analysis of the model's performance on the CPSC dataset for each type of abnormality. The analysis is limited to the four abnormalities shared between the CPSC and TNMG datasets.

6.2 Fine-tuning Results

After completing the full training process, the models undergo the μ-Fine-tuning process, where they are fine-tuned on a balanced subset of the CPSC dataset consisting of 1,000 samples. During this process, the weights in the middle S4D layer are static, while the weights in the encoder and decoder are adjusted to adapt to the new data. Following 50 epochs of fine-tuning, the models are tested again on the CPSC dataset to evaluate changes in performance. The fine-tuning process for various models trained using different combinations of full training and μ-Training is illustrated in Fig. 8.
The fine-tuned models are also tested on the TNMG test set to assess their performance on the original training data. Fig. 7b) summarizes the performance of the fine-tuned models. Table 5 presents a detailed breakdown of the fine-tuned models' performance on the TNMG test data, while Table 6 provides a detailed breakdown of their performance on the CPSC dataset.

6.3 Edge Deployment

To assess the effectiveness of this method for edge deployment, we conducted experiments using a model trained with a combination of half (150 epochs) full training and half (150 epochs) μ-Training. The model was deployed on the proposed Radxa Zero platform for on-device μ-Fine-Tuning. During the fine-tuning process, the system utilized a total of 3 GB of RAM, including 1.2 GB when idle, ensuring that the resources required for fine-tuning remained below 2 GB. The edge fine-tuned model was tested on the TNMG test set and the CPSC dataset. Its performance was compared to a model trained normally for 300 epochs and fine-tuned normally for 50 epochs on the same dataset performed on a GPU. The summarized results are presented in Table 7.

7 Discussion

The discussion will be structured to follow the order in which the results are presented in Section 6.

7.1 Impact on Training

We experimented with various combinations of full training and μ-Training. The key observation is that the combined approach performs nearly as well as standard full training, where the model completes 300 epochs of full training. Fig. 6, 7a), and Table 3 show that incorporating μ-Training alongside full training does not compromise the model's performance on the test data from the training dataset. This is particularly evident in metrics such as the average F1 score and AUROC, which reflect the balanced performance of the models. Notably, the optimal performance is achieved when the model undergoes more full training than μ-Training.
When the trained model was tested on the CPSC dataset, which serves as unseen data, its behavior closely mirrored the observations made during testing on the training dataset's test set. The models' performance did not significantly decline compared to those trained with the standard 300 epochs. As shown in Fig. 7a) and Table 4, the best performance was observed when the model underwent more full training than μ-Training.
Overall, the key observation is that models trained using a combination of full training and μ-Training maintain comparable performance to those trained using the standard process, in both in-sample and out-of-sample tests.

7.2 Impact on μ-Fine-Tuning

The impact of μ-Fine-tuning yields intriguing results. After fine-tuning, the model was tested again on both the test set of the trained TNMG dataset and the CPSC dataset. As shown in Fig. 8 and Fig. 7b), models trained through the standard training process alone did not perform as optimally as those that underwent a combination of full training and μ-Training. Models trained with both methods demonstrated better performance on the CPSC and the TNMG dataset's test set, indicating that they retain knowledge of the original data.
A closer examination of Table 5 and Table 6 provides additional support for the earlier inference. The standard trained model does not perform as optimally as the models trained using the combined approach, particularly in terms of F1 and AUROC, which assess the balanced performance of the model. These findings confirm

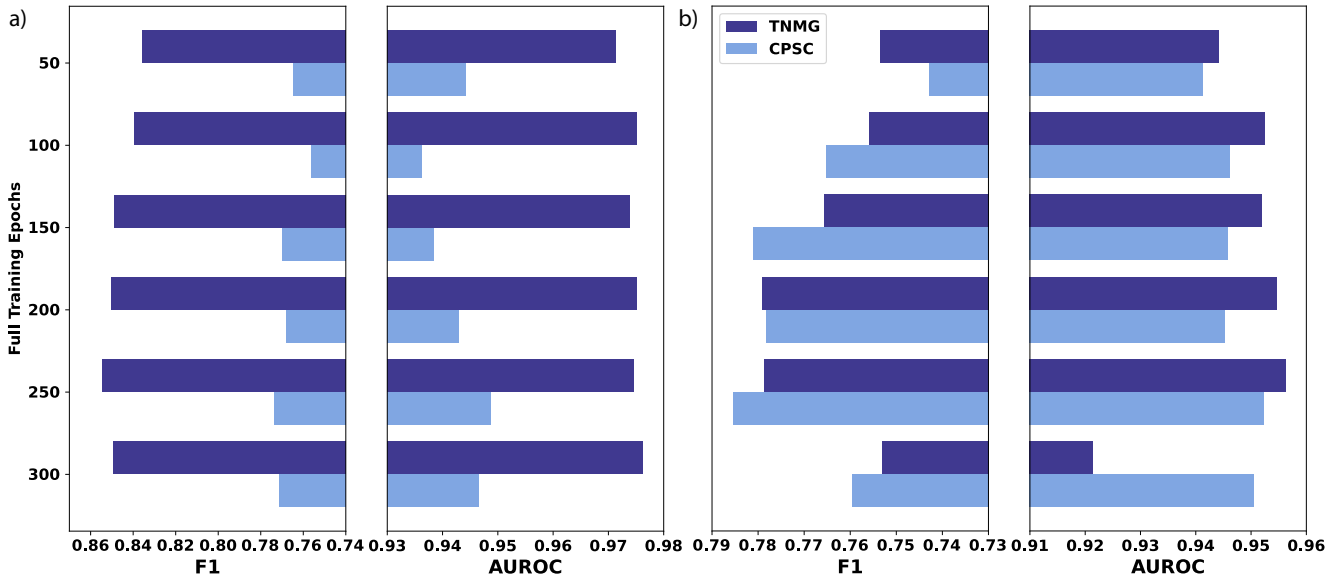

Figure 7: a) Test results of the μ-trained models on TNMG and CPSC datasets, with average F1 scores presented on the left and average AUROC scores on the right. The chart's legend in a) and b) are the same. b) Test results of the μ-fine-tuned models on TNMG and CPSC datasets, with average F1 scores on the left and average AUROC scores on the right.

Table 3: Models Tested on TNMG (P: Precision, R: Recall)

Class	P	R	F1	AUROC	P	R	F1	AUROC
	50 Full Training Epochs				**100 Full Training Epochs**			
1dAVb	57.22%	83.74%	67.99%	93.87%	58.99%	82.11%	68.66%	93.71%
RBBB	86.87%	92.87%	89.77%	97.79%	86.10%	94.82%	90.25%	98.69%
LBBB	87.58%	95.23%	91.24%	98.53%	87.38%	95.36%	91.19%	98.70%
SB	80.58%	95.29%	87.32%	98.25%	81.73%	94.44%	87.62%	98.48%
AF	66.45%	88.47%	75.90%	95.44%	66.56%	89.19%	76.23%	96.43%
ST	83.31%	95.88%	89.16%	98.91%	84.48%	95.43%	89.62%	99.09%
Average	77.00%	91.91%	83.56%	97.13%	77.54%	91.89%	83.93%	97.52%
	150 Full Training Epochs				**200 Full Training Epochs**			
1dAVb	59.91%	84.07%	69.96%	94.32%	60.42%	83.41%	70.08%	93.87%
RBBB	88.25%	94.25%	91.15%	97.77%	85.82%	94.71%	90.04%	98.69%
LBBB	88.72%	95.50%	91.98%	98.46%	88.47%	96.32%	92.23%	98.68%
SB	81.77%	96.01%	88.32%	98.98%	83.48%	96.58%	89.55%	98.59%
AF	68.78%	88.90%	77.56%	95.97%	69.86%	88.18%	77.96%	96.31%
ST	84.59%	97.10%	90.42%	98.85%	85.62%	95.27%	90.19%	98.92%
Average	78.67%	92.64%	84.90%	97.39%	78.95%	92.41%	85.01%	97.51%
	250 Full Training Epochs				**300 Full Training Epochs**			
1dAVb	61.72%	86.50%	72.04%	94.31%	60.96%	85.04%	71.01%	94.90%
RBBB	87.42%	93.56%	90.38%	98.14%	86.40%	93.56%	89.83%	98.64%
LBBB	89.24%	96.18%	92.58%	98.19%	87.36%	96.18%	91.56%	98.98%
SB	84.22%	94.44%	89.04%	98.55%	83.59%	94.44%	88.68%	98.39%
AF	68.59%	89.05%	77.49%	96.21%	68.88%	88.33%	77.40%	96.49%
ST	86.66%	96.04%	91.11%	99.40%	87.38%	94.97%	91.02%	98.34%
Average	79.64%	92.63%	85.44%	97.47%	79.09%	92.09%	84.92%	97.62%

that combining full training with μ-Training outperforms the standard training process when the models undergo μ-Fine-tuning with limited resource requirements on local edge devices.

7.3 Edge Deployment

To validate our proposed method, we deployed a model that is partially full trained and partially μ-Trained onto the Radxa Zero platform to test the effectiveness of μ-Fine-tuning. The experimental results are summarized in Table 7. Also included in the table are the performance metrics of the model that underwent traditional training and fine-tuning on a GPU. The results are noteworthy, as the models that underwent full training, μ-Training, and μ-Fine-tuning at the edge outperform the standard trained and fine-tuned model on the CPSC dataset. Interestingly, these models also perform better when tested on the training TNMG dataset. This demonstrates that

Table 4: Models Tested on CPSC (P: Precision, R: Recall)

Class	P	R	F1	AUROC	P	R	F1	AUROC
	50 Full Training Epochs				**100 Full Training Epochs**			
1dAVb	62.81%	86.57%	72.80%	94.07%	61.89%	84.35%	71.40%	93.26%
RBBB	89.48%	74.69%	81.42%	91.08%	91.44%	73.67%	81.60%	89.76%
LBBB	69.61%	90.25%	78.60%	97.72%	63.96%	90.25%	74.87%	95.91%
AF	60.47%	91.97%	72.97%	94.80%	62.14%	93.28%	74.59%	95.55%
Average	70.59%	85.87%	76.45%	94.42%	69.86%	85.39%	75.61%	93.62%
	150 Full Training Epochs				**200 Full Training Epochs**			
1dAVb	61.14%	88.92%	72.46%	93.64%	64.95%	85.73%	73.91%	93.18%
RBBB	91.63%	73.72%	81.71%	89.02%	91.74%	73.61%	81.69%	91.00%
LBBB	66.25%	88.98%	75.95%	96.52%	65.84%	89.83%	75.99%	97.15%
AF	67.65%	91.65%	77.84%	96.16%	63.93%	92.47%	75.59%	95.88%
Average	71.67%	85.82%	76.99%	93.84%	71.62%	85.41%	76.79%	94.30%
	250 Full Training Epochs				**300 Full Training Epochs**			
1dAVb	62.78%	88.09%	73.31%	93.97%	61.88%	86.57%	72.17%	95.19%
RBBB	92.17%	74.21%	82.22%	92.60%	91.28%	75.50%	82.64%	90.25%
LBBB	67.08%	90.68%	77.12%	97.18%	70.06%	87.29%	77.74%	97.21%
AF	65.59%	92.71%	76.82%	95.77%	64.44%	92.47%	75.95%	95.96%
Average	71.91%	86.42%	77.37%	94.88%	71.91%	85.45%	77.12%	94.65%

Table 5: Fine-tuned Models Tested on TNMG (P: Precision, R: Recall)

Class	P	R	F1	AUROC	P	R	F1	AUROC
	50 Full Training Epochs				**100 Full Training Epochs**			
1dAVb	60.57%	65.20%	62.80%	87.84%	63.43%	73.33%	68.02%	90.62%
RBBB	51.10%	93.90%	66.18%	95.50%	51.87%	94.13%	66.88%	95.72%
LBBB	90.80%	90.18%	90.49%	97.80%	91.97%	92.22%	92.10%	97.83%
SB	87.77%	86.02%	86.89%	96.69%	58.24%	93.72%	71.84%	96.20%
AF	47.22%	86.89%	61.19%	91.40%	56.16%	86.74%	68.18%	93.62%
ST	79.05%	90.85%	84.54%	97.21%	83.15%	90.24%	86.55%	97.46%
Average	69.42%	85.51%	75.35%	94.41%	67.47%	88.40%	75.60%	95.24%
	150 Full Training Epochs				**200 Full Training Epochs**			
1dAVb	69.13%	65.53%	67.28%	90.55%	64.89%	69.43%	67.09%	90.62%
RBBB	49.15%	93.67%	64.48%	95.13%	52.61%	91.60%	66.83%	94.35%
LBBB	92.39%	91.13%	91.76%	97.53%	90.22%	90.59%	90.40%	97.08%
SB	74.66%	93.72%	83.11%	98.38%	73.73%	94.86%	82.97%	97.27%
AF	60.74%	84.73%	70.76%	94.03%	59.59%	88.62%	71.26%	95.27%
ST	74.20%	91.62%	81.99%	95.56%	85.00%	93.29%	88.95%	98.21%
Average	70.05%	86.73%	76.56%	95.20%	71.01%	88.07%	77.92%	95.46%
	250 Full Training Epochs				**300 Full Training Epochs**			
1dAVb	78.21%	65.37%	71.21%	90.85%	65.98%	67.48%	66.72%	91.31%
RBBB	55.98%	91.60%	69.49%	94.68%	53.72%	92.98%	68.10%	94.33%
LBBB	90.82%	91.81%	91.32%	97.61%	85.63%	94.27%	89.74%	98.58%
SB	72.65%	93.58%	81.80%	98.28%	94.32%	63.91%	76.19%	81.32%
AF	56.73%	88.62%	69.18%	94.11%	52.63%	88.04%	65.88%	92.94%
ST	78.45%	91.01%	84.26%	98.23%	88.63%	82.01%	85.19%	94.30%
Average	72.14%	87.00%	77.88%	95.63%	73.48%	81.45%	75.30%	92.13%

our proposed method not only achieves superior results when computational power and memory are constrained through μ-training and fine-tuning, but also outperforms traditional training and fine-tuning processes.

8 Limitations and Future Works

Despite the promising results of the proposed methodology, several limitations warrant discussion. First, while the TDSSM model demonstrates lightweight characteristics and high efficiency, its applicability may be constrained to specific types of bio-signal data, such as ECG signals. The generalizability of the proposed technique to other bio-signal modalities or medical applications remains uncertain. Future work could extend the experimental framework to include additional datasets, such as those for electroencephalogram (EEG) or photoplethysmography (PPG) signals, to validate the versatility of the approach.

Another limitation lies in the computational resources and hardware employed for on-device fine-tuning. While the Radxa Zero was chosen for its resource-efficient design, the experimental results may not fully capture the constraints imposed by other edge devices with differing architectures or lower processing capabilities. Testing the methodology across a broader range of hardware platforms could offer deeper insights into its practicality and scalability for diverse deployment environments.

The μ-Training and μ-Fine-Tuning processes, although effective in improving the model's adaptability and reducing computational overhead, rely heavily on optimal hyperparameter configurations, such as the allocation of

Table 6: Fine-tuned Models Tested on CPSC (P: Precision, R: Recall)

Class	P	R	F1	AUROC	P	R	F1	AUROC
	50 Full Training Epochs				**100 Full Training Epochs**			
1dAVb	71.19%	74.60%	72.86%	91.46%	72.53%	79.36%	75.79%	92.60%
RBBB	66.61%	88.10%	75.86%	93.31%	68.68%	89.39%	77.68%	93.37%
LBBB	79.92%	84.32%	82.06%	97.16%	78.99%	86.02%	82.35%	96.83%
AF	51.06%	94.68%	66.34%	94.59%	56.02%	94.10%	70.23%	95.67%
Average	68.04%	84.57%	74.28%	94.13%	69.06%	87.22%	76.51%	94.62%
	150 Full Training Epochs				**200 Full Training Epochs**			
1dAVb	73.34%	79.64%	76.36%	92.62%	69.92%	81.44%	75.24%	92.78%
RBBB	65.89%	91.55%	76.63%	94.37%	70.79%	87.83%	78.39%	92.99%
LBBB	82.64%	84.75%	83.68%	95.48%	80.71%	86.86%	83.67%	96.51%
AF	64.23%	92.22%	75.72%	95.85%	61.31%	93.20%	73.97%	95.79%
Average	71.53%	87.04%	78.10%	94.58%	70.68%	87.33%	77.82%	94.52%
	250 Full Training Epochs				**300 Full Training Epochs**			
1dAVb	77.75%	81.30%	79.49%	93.77%	71.73%	79.78%	75.54%	94.60%
RBBB	72.31%	89.71%	80.08%	94.75%	62.36%	91.44%	74.15%	93.89%
LBBB	77.95%	83.90%	80.82%	96.39%	78.16%	86.44%	82.09%	97.59%
AF	60.55%	94.51%	73.81%	96.00%	58.61%	93.37%	72.02%	94.11%
Average	72.14%	87.36%	78.55%	95.23%	67.72%	87.76%	75.95%	94.60%

Table 7: Comparison of μ-Training and on-device μ-Fine-Tuning vs. Normal Training and Fine-Tuning Process (P: Precision, R: Recall)

Class	P	R	F1	AUROC	P	R	F1	AUROC
Tested on TNMG Dataset								
	μ-Trained and μ-Fine-tuned				**Standard Trained and Fine-tuned**			
1dAVb	68.93%	67.80%	68.36%	91.14%	75.95%	48.78%	59.41%	86.35%
RBBB	47.97%	92.41%	63.15%	93.66%	53.71%	93.33%	68.18%	94.40%
LBBB	91.83%	91.95%	91.88%	97.99%	87.78%	92.09%	89.88%	98.10%
SB	71.41%	97.29%	82.37%	98.50%	94.23%	74.61%	83.28%	90.64%
AF	60.52%	86.60%	71.25%	94.02%	60.31%	84.29%	70.31%	93.12%
ST	91.16%	84.91%	87.92%	93.93%	54.62%	98.17%	70.19%	98.36%
Average	71.97%	86.83%	77.49%	94.87%	71.10%	81.88%	73.54%	93.50%
Tested on CPSC Dataset								
	μ-Trained and μ-Fine-tuned				**Standard Trained and Fine-tuned**			
1dAVb	72.14%	82.13%	76.81%	93.18%	80.45%	64.96%	71.88%	90.90%
RBBB	64.95%	91.71%	76.04%	94.37%	70.04%	90.90%	79.12%	94.35%
LBBB	80.71%	86.86%	83.67%	95.70%	79.28%	84.32%	81.72%	96.24%
AF	59.62%	92.87%	72.62%	95.48%	58.57%	91.48%	71.42%	94.67%
Average	69.36%	88.39%	77.29%	94.68%	72.09%	82.92%	76.04%	94.04%

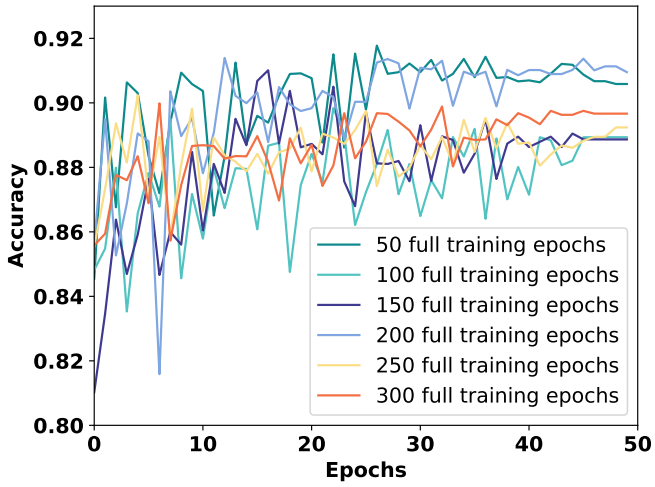

Figure 8: The accuracy evaluation throughout the entire fine-tuning process for various combinations of full training and μ-Training.

epochs between phases. The lack of a standardized approach for determining these configurations introduces a degree of subjectivity that may impact reproducibility. Future research could explore automated hyperparameter optimization techniques.

The design of the TDSSM model was adopted from prior work [8], and it was not explicitly designed to accommodate the proposed methodology. This inherent limitation suggests that the efficiency of the proposed μ-Training and μ-Fine-Tuning techniques may not be optimal, as the design of the encoder and decoder layers, along with the distribution of weights across layers, could significantly influence the effectiveness of the strategy. Future work could involve redesigning the model architecture to optimize the number of weights and layer structure to better align with the proposed methodology. Such refinements could enhance both the computational efficiency and overall performance of the technique, providing a more robust framework for bio-signal data analysis.

The proposed method may also apply to other tinyML models beyond the TDSSM tested in this study. This technique can be extended to other application domains,

particularly in conjunction with the growing adoption of IoT. Such expansion could enable broader real-world applications, subject to further testing and experimentation.

9 Conclusion

In conclusion, this study introduces a novel approach to training and fine-tuning deep learning models for bio-signal analysis, using the TDSSM model as a demonstrative example. By combining full training with μ-Training, we demonstrate that the model can achieve comparable performance to standard training while significantly reducing computational overhead. Including μ-Fine-Tuning further enhances the model's ability to adapt to new data with minimal resource consumption, making it well-suited for edge deployment in resource-constrained environments. The results from both the TNMG and CPSC datasets support the effectiveness of the combined approach, highlighting its potential for generalization and performance improvement. Our experiments also show that deploying the model on the Radxa Zero platform for edge μ-Fine-Tuning yields superior results compared to traditional training and fine-tuning processes, offering a compelling solution for real-time bio-signal processing. However, future work should investigate the applicability of this method to other bio-signal types, explore automated hyperparameter optimization techniques, and test the approach on a broader range of hardware platforms to further assess its scalability and robustness. With the potential integration of tinyML and IoT, the proposed method could also be beneficial to other models with broader applications outside the medical domain.

10 Acknowledgement

Zhaojing Huang gratefully acknowledges the support the Australian Government's Research Training Program (RTP) provides.

11 Availability of Data

This research paper uses the public CPSC dataset but acknowledges that the TNMG dataset is private and requires permission from its owner for access.

12 Conflict of Interest Statement

Authors affirm that they do not have any conflicts of interest, whether financial or non-financial, to disclose.

References

[1] Bing Shi and Yiming Wu. Task offloading and resource allocation strategies among multiple edge servers. *IEEE Internet of Things Journal*, 11(8): 14647–14656, 2023.

[2] Nduma N Basil, Solomon Ambe, Chukwuyem Ekhator, and Ekokobe Fonkem. Health records database and inherent security concerns: A review of the literature. *Cureus*, 14(10), 2022.

[3] Mansoor Ali, Faisal Naeem, Muhammad Tariq, and Georges Kaddoum. Federated learning for privacy preservation in smart healthcare systems: A comprehensive survey. *IEEE Journal of Biomedical and Health Informatics*, 27(2):778–789, 2022.

[4] Ligeng Zhu, Zhijian Liu, and Song Han. Deep leakage from gradients. *Advances in Neural Information Processing Systems*, 32, 2019.

[5] Franziska Boenisch, Adam Dziedzic, Roei Schuster, Ali Shahin Shamsabadi, Ilia Shumailov, and Nicolas Papernot. Reconstructing individual data points in federated learning hardened with differential privacy and secure aggregation. In *IEEE 8th European Symposium on Security and Privacy (EuroS&P)*, pages 241–257, 2023.

[6] An Wang, Jiong Yu, Danqi Liu, and Yong Cui. A measurement study for transmission energy on mobile device. In *Proceedings of 2012 2nd International Conference on Computer Science and Network Technology*, pages 708–714. IEEE, 2012.

[7] Zhaojing Huang, Leping Yu, Luis Fernando Herbozo Contreras, Kamran Eshraghian, Nhan Duy Truong, Armin Nikpour, and Omid Kavehei. Advancing privacy-aware machine learning on sensitive data via edge-based continual μ-training for personalized large models. *Machine Learning: Science and Technology*, 2025.

[8] Zhaojing Huang, Wing Hang Leung, Jiashuo Cui, Leping Yu, Luis Fernando Herbozo Contreras, Nhan Duy Truong, Armin Nikpour, and Omid Kavehei. Cardiac abnormality detection with a tiny diagonal state space model based on sequential liquid neural processing unit. *APL Machine Learning*, 2(2), 2024.

[9] Polychronis E Dilaveris and Harold L Kennedy. Silent atrial fibrillation: epidemiology, diagnosis, and clinical impact. *Clinical Cardiology*, 40(6):413–418, 2017.

[10] Ayodeji Oseni, Nour Moustafa, Helge Janicke, Peng Liu, Zahir Tari, and Athanasios Vasilakos. Security and privacy for artificial intelligence: Opportunities and challenges. *arXiv preprint arXiv:2102.04661*, 2021.

[11] Lachit Dutta and Swapna Bharali. TinyML meets IoT: A comprehensive survey. *Internet of Things*, 16:100461, 2021.

[12] Zhaojing Huang, Luis Fernando Herbozo Contreras, Leping Yu, Nhan Duy Truong, Armin Nikpour, and Omid Kavehei. S4D-ECG: A shallow state-of-the-art model for cardiac abnormality classification. *Cardiovascular Engineering and Technology*, pages 1–12, 2024.

[13] Albert Gu, Karan Goel, Ankit Gupta, and Christopher Ré. On the parameterization and initialization of diagonal state space models. *Advances in Neural Information Processing Systems*, 35:35971–35983, 2022.

[14] Zhaojing Huang, Luis Fernando Herbozo Contreras, Wing Hang Leung, Leping Yu, Nhan Duy Truong, Armin Nikpour, and Omid Kavehei. Efficient edge-AI models for robust ECG abnormality detection on resource-constrained hardware. *Journal of Cardiovascular Translational Research*, pages 1–14, 2024.

[15] Mathias Lechner, Ramin Hasani, Alexander Amini, Thomas A Henzinger, Daniela Rus, and Radu Grosu. Neural circuit policies enabling auditable autonomy. *Nature Machine Intelligence*, 2(10):642–652, 2020.

[16] Zhaojing Huang, Wing Hang Leung, Leping Yu, Luis Fernando Herbozo Contreras, Ziyao Zhang, Nhan Duy Truong, Armin Nikpour, and Omid Kavehei. On-device edge-learning for cardiac abnormality detection using a bio-inspired and spiking shallow network. *APL Machine Learning*, 2(2), 2024.

[17] Ziming Liu, Yixuan Wang, Sachin Vaidya, Fabian Ruehle, James Halverson, Marin Soljačić, Thomas Y. Hou, and Max Tegmark. KAN: Kolmogorov-arnold networks, 2024.

[18] Zhaojing Huang, Jiashuo Cui, Leping Yu, Luis Fernando Herbozo Contreras, and Omid Kavehei. Abnormality detection in time-series bio-signals using kolmogorov-arnold networks for resource-constrained devices. *medRxiv*, pages 2024–06, 2024.

[19] Li Li, Yuxi Fan, Mike Tse, and Kuo-Yi Lin. A review of applications in federated learning. *Computers & Industrial Engineering*, 149:106854, 2020.

[20] Massimo Merenda, Carlo Porcaro, and Demetrio Iero. Edge machine learning for AI-enabled IoT devices: A review. *Sensors*, 20(9):2533, 2020.

[21] Antônio H Ribeiro, Manoel Horta Ribeiro, Gabriela MM Paixão, Derick M Oliveira, Paulo R Gomes, Jéssica A Canazart, Milton PS Ferreira, Carl R Andersson, Peter W Macfarlane, Wagner Meira Jr, et al. Automatic diagnosis of the 12-lead ECG using a deep neural network. *Nature Communications*, 11(1):1760, 2020.

[22] Feifei Liu, Chengyu Liu, Lina Zhao, Xiangyu Zhang, Xiaoling Wu, Xiaoyan Xu, Yulin Liu, Caiyun Ma, Shoushui Wei, Zhiqiang He, et al. An open access database for evaluating the algorithms of electrocardiogram rhythm and morphology abnormality detection. *Journal of Medical Imaging and Health Informatics*, 8(7):1368–1373, 2018.

[23] Euan A Ashley and Josef Niebauer. Arrhythmia. In *Cardiology explained*. Remedica, 2004.

[24] Kenneth A Mayuga, Artur Fedorowski, Fabrizio Ricci, Rakesh Gopinathannair, Jonathan Walter Dukes, Christopher Gibbons, Peter Hanna, Dan Sorajja, Mina Chung, David Benditt, et al. Sinus tachycardia: a multidisciplinary expert focused review. *Circulation: Arrhythmia and Electrophysiology*, 15(9):e007960, 2022.

[25] Sunjeet Sidhu and Joseph E Marine. Evaluating and managing bradycardia. *Trends in cardiovascular medicine*, 30(5):265–272, 2020.

[26] Nicholas Y Tan, Chance M Witt, Jae K Oh, and Yong-Mei Cha. Left bundle branch block: current and future perspectives. *Circulation: Arrhythmia and Electrophysiology*, 13(4):e008239, 2020.

[27] AK Agarwal and P Venugopalan. Right bundle branch block: varying electrocardiographic patterns.: Aetiological correlation, mechanisms and electrophysiology. *International journal of cardiology*, 71(1):33–39, 1999.

[28] Yoshihiro Tanaka, Ravi B Patel, Hayato Tada, Kenshi Hayashi, Masayuki Takamura, Masa-aki Kawashiri, and Philip Greenland. First-degree atrioventricular block is associated with incident atrial fibrillation in the japanese general population aged $\geq$ 40 years. *Circulation*, 142(Suppl_3):A13015–A13015, 2020.

[29] Zhaojing Huang, Sarisha MacLachlan, Leping Yu, Luis Fernando Herbozo Contreras, Nhan Duy Truong, Antonio Horta Ribeiro, and Omid Kavehei. Generalization challenges in electrocardiogram deep learning: insights from dataset characteristics and attention mechanism. *Future Cardiology*, pages 1–12, 2024.